ELSEVIER

www.elsevier.nl/locate/jorganchem

Journal of Organometallic Chemistry 598 (2000) 353–358

Journal of Organometallic Chemistry

Syntheses, characterization and structures of chromium group carbonyl complexes containing a multifunctional $Ph_2P(o\text{-}C_6H_4)CH{=}N(CH_2)_2(o\text{-}C_6H_4N)$ ligand

Ching-Chao Yang [a], Wen-Yann Yeh [a,*], Gene-Hsiang Lee [b], Shie-Ming Peng [b]

[a] *Department of Chemistry, National Sun Yat-Sen University, Kaohsiung 804, Taiwan*
[b] *Department of Chemistry, National Taiwan University, Taipei 106, Taiwan*

Received 24 September 1999; received in revised form 15 November 1999; accepted 22 November 1999

Abstract

Reactions of the phosphine–imine–pyridine-containing ligand $Ph_2P(o\text{-}C_6H_4)CH{=}N(CH_2)_2(o\text{-}C_6H_4N)$ (PNN) with $M(CO)_3(NCMe)_3$ (M = Cr, Mo, W) produce the tridentate complexes *fac*-$M(CO)_3(\eta^3\text{-PNN})$. On the other hand, treating $W(CO)_4(NCMe)_2$ with PNN results in the bidentate complex $W(CO)_4(\eta^2\text{-PNN})$, which converts to *fac*-$W(CO)_3(\eta^3\text{-PNN})$ upon heating, but no facial → meridional isomerism is evidenced. The new compounds have been characterized by elemental analysis and mass, IR, and NMR spectroscopy. The molecular structures of $W(CO)_4(\eta^2\text{-PNN})$, *fac*-$W(CO)_3(\eta^3\text{-PNN})$ and *fac*-$Mo(CO)_3(\eta^3\text{-PNN})$ are determined by an X-ray diffraction study.

Keywords: Chromium group; Multifunctional ligand

1. Introduction

The multifunctional compound $Ph_2P(o\text{-}C_6H_4)CH{=}N(CH_2)_2(o\text{-}C_6H_4N)$ (PNN), which contains a phosphine, an imine and a pyridyl electron-donating groups, was prepared by Lavery and Nelson from co-condensation of $Ph_2P(o\text{-}C_6H_4)C(=O)H$ and $H_2N(CH_2)_2(o\text{-}C_6H_4N)$ [1]. Due to its flexible structure, this molecule can act either as a monodentate P, a bidentate P–N or a tridentate P–N–N ligand, which is applicable to the design of new catalytic reactions [2–5]. For instance, the hemilabile property of the pyridyl group has made the $[(PNN)Pd(allyl)]^+$ complexes very active in allylic alkylation reactions [6].

We recently found the reactions of PNN with triosmium carbonyl clusters to afford complexes containing chelate and bridging PNN ligands as well as leading to C–H and C–P bond activation of the PNN ligand [7]. In the present research, we explore the reactions of PNN with mononuclear chromium group carbonyl complexes.

2. Results and discussion

2.1. Syntheses

Reactions of $M(CO)_3(NCMe)_3$ with the PNN molecule at room temperature result in a facile substitution of the labile acetonitrile ligands to afford *fac*-$M(CO)_3(\eta^3\text{-PNN})$ in 52, 70 and 72% yields for M = Cr, Mo and W, respectively (Eq. (1)). On the other hand, treating $W(CO)_4(NCMe)_2$ with PNN produces the phosphine–imine bidentate complex $W(CO)_4(\eta^2\text{-PNN})$, which transforms to *fac*-$W(CO)_3(\eta^3\text{-PNN})$ upon heating (Eq. (2)). The Pd(0), Pd(II) and Pt(II) complexes containing η^1–η^3-PNN ligands were prepared previously by Vrieze and coworkers [4,8], while the $Mo(CO)_4$ complexes with the related P–N and P–N–N–P ligands were reported by Rauchfuss [9].

* Corresponding author. Fax: +886-7-5253908.
E-mail address: wenyann@mail.nsysu.edu.tw (W.-Y. Yeh)

0022-328X/00/$ - see front matter
PII: S0022-328X(99)00734-2

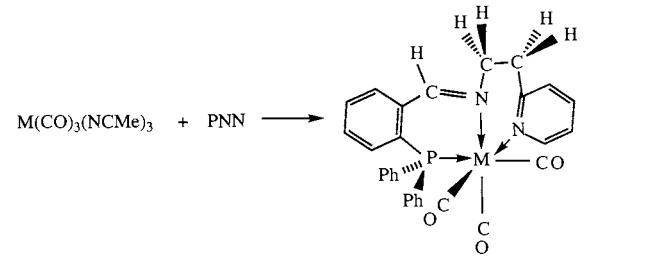

(1)

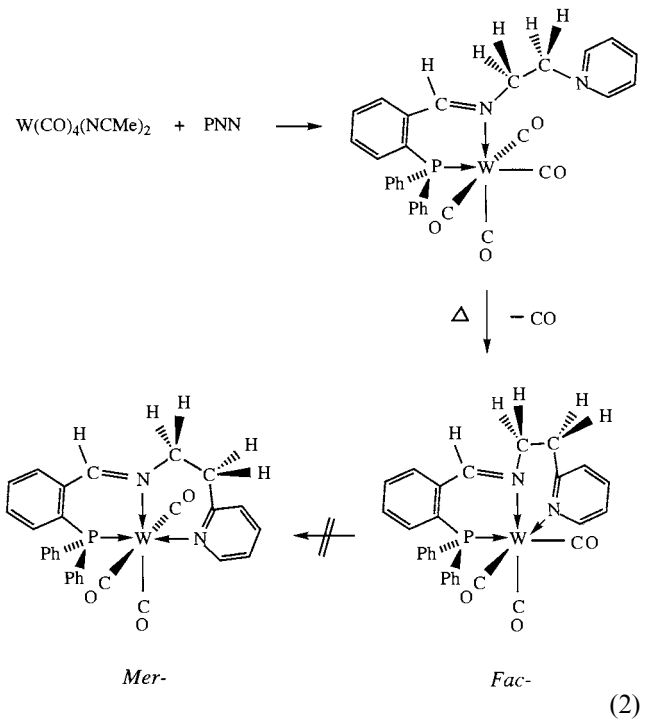

(2)

Attempts to synthesize the tungsten poly(PNN) complexes, such as $W(CO)_4(PNN)_2$, $W(CO)_3(PNN)_2$ or $W(CO)_3(PNN)_3$, have been unsuccessful. It was found that treating $W(CO)_3(NCMe)_3$ with an excess amount of PNN, heating or photolysis of $W(CO)_4(\eta^2$-PNN) in the presence of PNN, or pyrolysis of $W(CO)_6$ and PNN at high temperature led only to *fac*-$W(CO)_3(\eta^3$-PNN). Since both the P–N and N–N sets of the ligand can form a stable six-membered chelate ring upon coordination, it is probable that the chelate effect [10] is governing the products yielded.

The d^6 metal tricarbonyl complexes $M(CO)_3L_3$ exhibit facial (*fac*) and meridional (*mer*) isomers. When L is a good σ donor and poor π acceptor relative to CO, the *fac* isomer is expected to be more stable electronically to achieve stronger M–CO back donation. On the other hand, the *mer* isomer is less sterically encumbered and is favored when L contains bulky groups [11,12]. For example, only *fac*-$W(CO)_3(PMe_3)_3$ is existent while both *fac*-$W(CO)_3(PPh_3)_3$ and *mer*-$W(CO)_3(PPh_3)_3$ are present [13]. We were unable to convert *fac*-$W(CO)_3(\eta^3$-PNN) into *mer*-$W(CO)_3(\eta^3$-PNN) thermally. Previous investigation on the transformation of *fac*-$W(CO)_3(\eta^2$-dppf)(η^1-dppm) to *mer*-$W(CO)_3(\eta^2$-dppm)(η^1-dppf) suggested a pathway through opening of the chelated diphosphine ligand [13]. Since the flexible PNN ligand reveals little ring constraint, the inaccessible *fac* → *mer* isomerism is probably due to the electronic effect.

2.2. Characterization of new compounds

Complexes *fac*-$M(CO)_3(\eta^3$-PNN) (M = Cr, Mo, W) form air-stable, dark red crystals. Their FAB mass spectra exhibit molecular ion peaks at $m/z = 530$, 574 and 662 for ^{52}Cr, ^{96}Mo and ^{184}W, respectively, and fragments resulting from successive loss of three CO groups. The IR spectra in the carbonyl-stretching region for these complexes are similar, suggesting great resemblance of their structures.

The ^{1}H-NMR spectrum of free PNN in $CDCl_3$ presents a doublet resonance at 9.01 ppm ($J_{P-H} = 5$ Hz) for the CH=N proton and two 2H triplets at 3.93 and 3.04 ppm ($J_{H-H} = 7$ Hz) for the $(CH_2)_2$ protons, while its $^{31}P\{^1H\}$-NMR spectrum shows a singlet at −13.08 ppm for the phosphine group. In the *fac*-$M(CO)_3(\eta^3$-PNN) complexes, the phosphine ^{31}P resonances are shifted downfield to 50.94, 36.13 and 31.73 ppm for M = Cr, Mo and W, respectively, and the imine CH=N ^{1}H resonances are shifted slightly to ca. 9.5 ppm. It has been noted that, for the metal phosphine complexes of a similar structure, one generally observes a high-field shift of the ^{31}P resonance as one descends in a given group [14]. Furthermore, the $(CH_2)_2$ proton resonances are split into four 1H multiplets in the range 4.30–1.13 ppm to indicate asymmetric coordination of the PNN ligand, leading to diastereotopic methylene groups.

$W(CO)_4(\eta^2$-PNN) forms orange–red crystals. Its FAB mass spectrum displays a molecular ion peak at $m/z = 690$ for ^{184}W, which is 28 more than that of *fac*-$W(CO)_3(\eta^3$-PNN), and fragments corresponding to successive loss of four carbonyls. Apparently, either the P–N or the N–N set of PNN ligand is bonded to the W atom to satisfy the 18-electron rule. On the basis of the ^{31}P-NMR spectrum, which displays a resonance at 24.19 ppm with ^{183}W satellites ($^1J_{W-P} = 238$ Hz), the P–N coordination mode is preferred. The IR spectra of $W(CO)_4(\eta^2$-PNN) and *fac*-$W(CO)_3(\eta^3$-PNN) in the carbonyl region are shown in Fig. 1; it appears that the absorptions are shifted to lower energy with increasing substitution, consistent with the stronger net donor capability of the PNN ligand compared with CO.

2.3. Molecular structures

Crystals of $W(CO)_4(\eta^2$-PNN), *fac*-$W(CO)_3(\eta^3$-PNN) and *fac*-$Mo(CO)_3(\eta^3$-PNN) contain an ordered array of discrete monomeric molecular units, which are mutu-

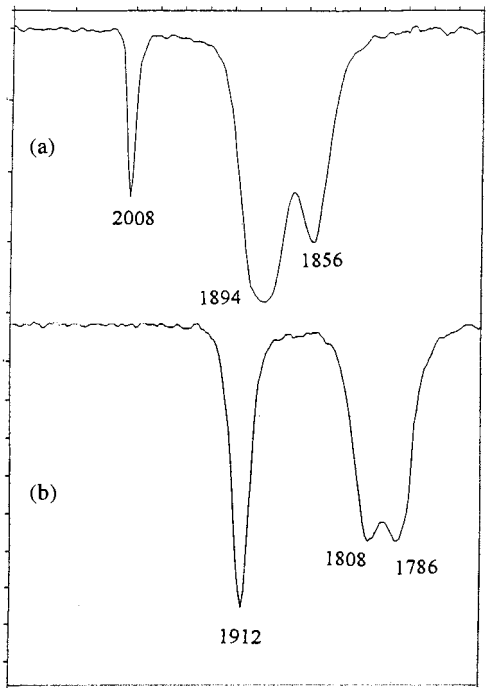

Fig. 1. IR spectra in the carbonyl region for (a) $W(CO)_4(\eta^2$-PNN) and (b) *fac*-$W(CO)_3(\eta^3$-PNN) obtained in CH_2Cl_2 solvent.

ally separated by normal van der Waals distances. Their ORTEP diagrams are shown in Figs. 2–4. Selected bond distances and bond angles for $W(CO)_4(\eta^2$-PNN) are given in Table 1, and for *fac*-$W(CO)_3(\eta^3$-PNN) and *fac*-$Mo(CO)_3(\eta^3$-PNN) are collected in Table 2.

$W(CO)_4(\eta^2$-PNN) is associated with four terminal carbonyls with the W–C–O angles in the range 174.7(4)–178.2(4)°. The W–CO distances are 2.024(4) Å to C(2) and 2.007(4) Å to C(4), while those distances *trans* to the phosphine and imine groups are slightly but significantly shorter, being 1.982(4) Å to C(3) and

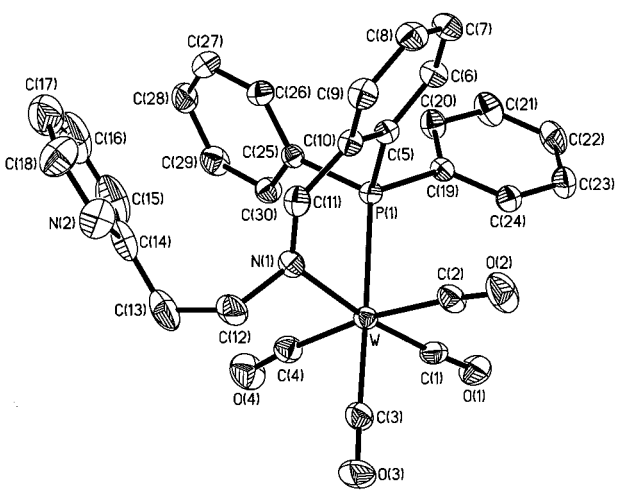

Fig. 2. Molecular structure of $W(CO)_4(\eta^2$-PNN). Thermal ellipsoids are drawn at 30% probability. The hydrogen atoms have been artificially omitted for clarity.

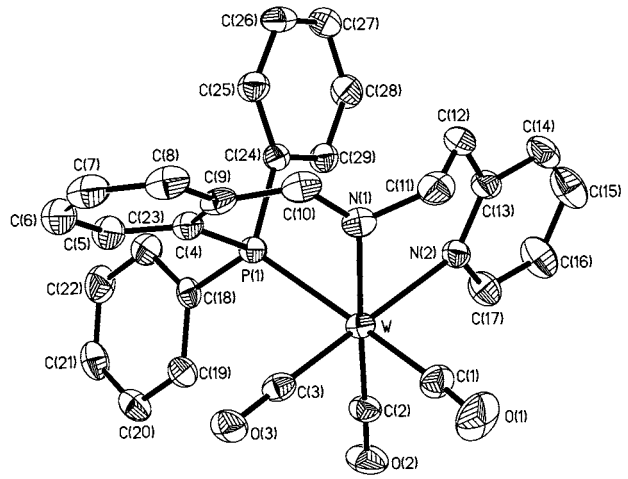

Fig. 3. Molecular structure of *fac*-$W(CO)_3(\eta^3$-PNN). Thermal ellipsoids are drawn at 30% probability. The hydrogen atoms have been artificially omitted for clarity.

1.955(4) Å to C(1). Enhancement of W→CO back-donation for the latter two bondings is consistent with good σ donor and poor π acceptor of the phosphine (and imine) ligand relative to CO. The PNN ligand chelates the tungsten atom through the phosphine–imine groups with the bite angle P(1)–W–N(1) = 80.74(2)°. The uncoordinated C(11)–N(1) bond (1.275(5) Å) retains a C=N double-bond character.

The molecular structures of *fac*-$W(CO)_3(\eta^3$-PNN) and *fac*-$Mo(CO)_3(\eta^3$-PNN) are essentially identical, where the coordination about the central metal atom is a distorted octahedron with the PNN ligand capping a triangular face. Three terminal carbonyl ligands are linked to W and Mo atoms with the M–CO distances in the range 1.927(5)–1.976(6) Å and the M–C–O angles in the range 175.3(6)–178.8(4)°. The P(1)–M–N(1), P(1)–M–N(2) and N(1)–M–N(2) angles are 79.1(1), 94.2(1) and 82.8(1)° for M = W, and 78.5(1), 94.55(9)

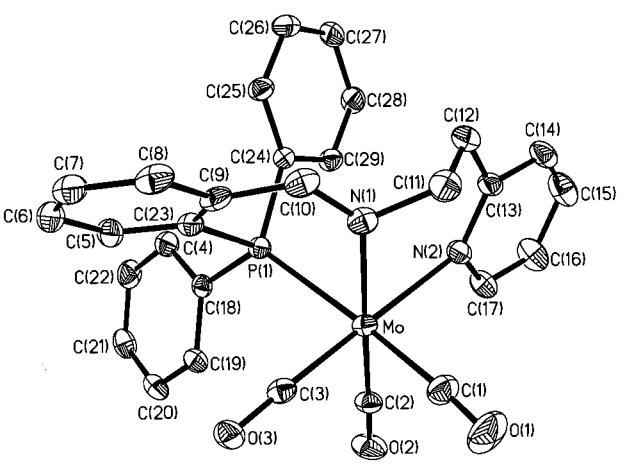

Fig. 4. Molecular structure of *fac*-$Mo(CO)_3(\eta^3$-PNN). Thermal ellipsoids are drawn at 30% probability. The hydrogen atoms have been artificially omitted for clarity.

Table 1
Selected bond distances (Å) and bond angles (°) for $W(CO)_4(\eta^2$-PNN)

Bond distances			
W–P(1)	2.485(1)	W–N(1)	2.272(3)
W–C(1)	1.955(4)	W–C(2)	2.025(4)
W–C(3)	1.982(4)	W–C(4)	2.007(4)
C(1)–O(1)	1.163(4)	C(2)–O(2)	1.142(5)
C(3)–O(3)	1.150(5)	C(4)–O(4)	1.148(5)
P(1)–C(5)	1.826(3)	C(5)–C(10)	1.401(5)
C(10)–C(11)	1.475(5)	C(11)–N(1)	1.275(5)
N(1)–C(12)	1.492(4)		
Bond angles			
W–C(1)–O(1)	176.9(3)	W–C(2)–O(2)	175.1(4)
W–C(3)–O(3)	178.2(4)	W–C(4)–O(4)	174.7(4)
P(1)–W–N(1)	80.74(7)	C(1)–W–N(1)	173.2(1)
C(3)–W–P(1)	175.6(1)	C(2)–W–C(4)	172.2(2)
C(11)–N(1)–C(12)	113.9(3)		

and 83.1(1)° for M = Mo. The P(1), C(4), C(9), C(10) and N(1) atoms are planar to within ± 0.1 Å for both compounds. The C(10)–N(1) double-bond distances are 1.281(7) and 1.276(6) Å for the W and Mo complexes, respectively. We note that the Mo–CO bonds are slightly shorter (av. 0.008 Å) than the W–CO bonds, while the M–P(1), M–N(1) and M–N(2) distances to the molybdenum atom are longer than those to the tungsten atom by 0.01–0.02 Å. Since the atomic sizes of Mo and W are comparable, this phenomenon might arise from electronic effects with different donor ability of the CO and PNN ligands and/or steric repulsions between the ligands.

Table 2
Selected bond distances (Å) and bond angles (°) for *fac*-$M(CO)_3(\eta^3$-PNN) (M = W and Mo)

	M = W	M = Mo
Bond distances		
M–P(1)	2.484(1)	2.494(1)
M–N(1)	2.228(4)	2.243(4)
M–N(2)	2.341(4)	2.364(4)
M–C(1)	1.976(6)	1.970(5)
M–C(2)	1.938(5)	1.931(4)
M–C(3)	1.940(5)	1.927(5)
C(1)–O(1)	1.144(6)	1.150(6)
C(2)–O(2)	1.171(6)	1.166(5)
C(3)–O(3)	1.163(6)	1.168(5)
P(1)–C(4)	1.837(5)	1.834(4)
C(4)–C(9)	1.410(7)	1.403(6)
C(9)–C(10)	1.456(8)	1.454(7)
C(10)–N(1)	1.281(7)	1.276(6)
N(1)–C(11)	1.461(7)	1.475(6)
C(11)–C(12)	1.508(8)	1.503(7)
C(12)–C(13)	1.492(8)	1.496(7)
C(13)–N(2)	1.345(6)	1.351(5)
Bond angles		
M–C(1)–O(1)	175.3(6)	175.6(5)
M–C(2)–O(2)	178.8(4)	178.2(4)
M–C(3)–O(3)	177.2(4)	176.2(4)
P(1)–M–N(1)	79.1(1)	78.5(1)
P(1)–M–N(2)	94.2(1)	94.55(9)
N(1)–M–N(2)	82.8(1)	83.1(1)
P(1)–M–C(1)	168.3(2)	168.6(2)
C(3)–M–N(2)	177.8(2)	177.9(2)
C(2)–M–N(1)	175.6(2)	175.9(2)
C(10)–N(1)–C(11)	115.4(4)	115.9(4)
N(1)–C(10)–C(9)	127.1(5)	126.2(4)

3. Experimental

3.1. General methods

All manipulations were carried out under an atmosphere of purified dinitrogen with standard Schlenk techniques [15]. $Cr(CO)_6$, $Mo(CO)_6$ and $W(CO)_6$ from Strem were used as received. Anhydrous Me_3NO was obtained from $Me_3NO{\cdot}2H_2O$ (Aldrich) by sublimation under vacuum twice. $Ph_2P(o\text{-}C_6H_4)CH{=}N(CH_2)_2(o\text{-}C_6H_4N)$ was synthesized from condensation of $Ph_2P(o\text{-}C_6H_4)C(=O)H$ and $NH_2(CH_2)_2(o\text{-}C_6H_4N)$ (Aldrich) as described in the literature [1]. Solvents were dried over appropriate reagents under dinitrogen and distilled immediately before use [16]. Infrared spectra were recorded with a 0.1 mm-path CaF_2 solution cell on a Hitachi I-2001 IR spectrometer. ^{1}H- and ^{31}P-NMR spectra were obtained on a Varian VXR-300 spectrometer at 300 and 121.4 MHz, respectively. Fast-atom-bombardment (FAB) mass spectra were recorded by using a VG Blotch-5022 mass spectrometer. Elemental analyses were performed at the National Science Council Regional Instrumentation Center at National Chung-Hsing University, Taichung, Taiwan.

3.2. Synthesis of *fac*-$Cr(CO)_3(\eta^3$-PNN)

A 50 ml Schlenk flask was equipped with a magnetic stir bar and a reflux condenser connected to an oil bubbler. $Cr(CO)_6$ (101 mg, 0.45 mmol) and acetonitrile (15 ml) were introduced into the flask under dinitrogen, and the solution was heated to reflux for 72 h, at which point the IR spectrum indicated $Cr(CO)_6$ was completely transformed to $Cr(CO)_3(NCMe)_3$. The acetonitrile solvent was then removed under vacuum. A solution of PNN (181 mg, 0.45 mmol) in dichloromethane (10 ml) was added to the flask by a syringe and the reaction mixture was stirred at ambient temperature for 1 h, resulting a solution color change from bright yellow to deep red. The solution was then dried under vacuum, and the crude product was crystallized from dichloromethane–hexane to afford dark red crystals of *fac*-$Cr(CO)_3(\eta^3$-PNN) (124 mg, 0.23 mmol, 52%). IR (CH_2Cl_2, ν_{CO}): 1914 s, 1810 s, 1788 s cm^{-1}.

^{1}H-NMR (C_6D_6, 20°C): 9.56 (d, CH=N), 8.07–5.90 (m, Ph, Py), 4.30 (m, 1H), 2,95 (m, 1H), 2.10 (m, 1H), 1.13 (m, 1H, CH_2) ppm. $^{31}P\{^1H\}$-NMR (C_6D_6, 20°C): 50.94 ppm. MS (FAB) m/z: 530 (M^+, ^{52}Cr), 530–28n ($n = 1$–3).

3.3. Synthesis of fac-Mo(CO)$_3$(η^3-PNN)

$Mo(CO)_6$ (100 mg, 0.37 mmol) and acetonitrile (15 ml) were refluxed under dinitrogen for 12 h to produce $Mo(CO)_3(NCMe)_3$. The reaction of $Mo(CO)_3(NCMe)_3$ and PNN (150 mg, 0.37 mmol) was then carried out and worked up in a fashion identical with that above. *fac*-$Mo(CO)_3(\eta^3$-PNN) (149 mg, 0.26 mmol, 70%) was obtained as dark red crystals after crystallization from dichloromethane–hexane. IR (CH_2Cl_2, ν_{CO}): 1920 s, 1816 s, 1794 s cm^{-1}. ^{1}H-NMR (C_6D_6, 20°C): 9.40 (d, CH=N), 8.05–5.95 (m, Ph, Py), 4.08 (m, 1H), 2,81 (m, 1H), 2.12 (m, 1H), 1.20 (m, 1H, CH_2) ppm. $^{31}P\{^1H\}$-NMR (C_6D_6, 20°C): 36.13 ppm. MS (FAB) m/z: 574 (M^+, ^{96}Mo), 574–28n ($n = 1$–3). Anal. Found C, 55.53; H, 3.65; N, 4.25. $C_{30}H_{25}Cl_2N_2O_3PMo$ (containing a CH_2Cl_2 crystal solvent) Anal. Calc. C, 54.64; H, 3.82; 4.24%.

3.4. Synthesis of fac-W(CO)$_3$(η^3-PNN)

$W(CO)_6$ (90 mg, 0.25 mmol) and acetonitrile (20 ml) were refluxed under dinitrogen for 72 h to produce $W(CO)_3(NCMe)_3$. The reaction of $W(CO)_3(NCMe)_3$ and PNN (101 mg, 0.25 mmol) was then carried out and worked up in a fashion identical with that above. *fac*-$W(CO)_3(\eta^3$-PNN) (119 mg, 0.18 mmol, 72%) was obtained as dark red crystals after crystallization from dichloromethane–hexane. IR (CH_2Cl_2, ν_{CO}): 1912 s, 1808 s, 1786 s cm^{-1}. ^{1}H-NMR (C_6D_6, 20°C): 9.45 (d, CH=N), 8.07–5.92 (m, Ph, Py), 4.03 (m, 1H), 3.93 (m, 1H), 2.89 (m, 1H), 1.20 (m, 1H, CH_2) ppm. $^{31}P\{^1H\}$-NMR (C_6D_6, 20°C): 31.73 (s, with ^{183}W satellites, $J_{W-P} = 227$ Hz) ppm. MS (FAB) m/z: 662 (M^+, ^{184}W), 662–28n ($n = 1$–3). Anal. Found C, 47.96; H, 3.54; N, 3.75. $C_{30}H_{25}Cl_2N_2O_3PW$ (containing a CH_2Cl_2 crystal solvent) Anal. Calc. C, 48.19; H, 3.34; 3.74%.

3.5. Synthesis of W(CO)$_4$(η^2-PNN)

$W(CO)_6$ (100 mg, 0.28 mmol) and dichloromethane (5 ml) were placed in a 50 ml Schlenk flask under dinitrogen. A solution of Me_3NO (45 mg, 0.60 mmol) in acetonitrile (7 ml) was added dropwise into the flask by a syringe over a period of 20 min. The mixture was stirred at ambient temperature for 2 h, at which point the IR spectrum indicated the presence of $W(CO)_4(NCMe)_2$. The acetonitrile solvent was then removed under vacuum. A solution of PNN (112 mg, 0.28 mmol) in dichloromethane (7 ml) was added to the flask by a syringe and the reaction mixture was stirred at ambient temperature for 1 h, resulting a solution color change from bright yellow to orange red. The volatile materials were removed under vacuum, and the residue was crystallized from dichloromethane–hexane to afford orange red crystals of $W(CO)_4(\eta^2$-PNN) (99 mg, 0.14 mmol, 50%). IR (CH_2Cl_2, ν_{CO}): 2008 s, 1894 s, 1856 s cm^{-1}. ^{1}H-NMR (C_6D_6, 20°C): 8.52 (d, CH=N), 8.07–6.85 (m, Ph, Py), 4.35 (t, 2H, CH_2), 3.11 (t, 2H, CH_2) ppm. $^{31}P\{^1H\}$-NMR (C_6D_6, 20°C): 24.19 (s, with ^{183}W satellites, $J_{W-P} = 238$ Hz) ppm. MS (FAB) m/z: 690 (M^+, ^{184}W), 690–28n ($n = 1$–4). Anal. Found C, 52.12; H, 3.44; N, 4.00. $C_{30}H_{23}N_2O_4PW$; Anal. Calc. C, 52.19; H, 3.35; 4.05%.

3.6. Thermolysis of W(CO)$_4$(η^2-PNN)

A solution of $W(CO)_4(\eta^2$-PNN) (9 mg) in n-octane (4 ml) was heated to reflux under dinitrogen for 2 h, resulting in a solution color change from orange red to deep red. The octane solvent was removed under vacuum, and the residue crystallized from dichloromethane–hexane to yield *fac*-$W(CO)_3(\eta^3$-PNN) (6 mg).

Similar results were obtained by heating $W(CO)_4(\eta^2$-PNN) in the presence of PNN ligand. There was no evidence for the formation of $W(CO)_3(PNN)_2$ or $W(CO)_4(PNN)_2$.

3.7. Attempts to isomerize fac-W(CO)$_3$(η^3-PNN) to mer-W(CO)$_3$(η^3-PNN) thermally

A solution of *fac*-$W(CO)_3(\eta^3$-PNN) (5 mg) in toluene solvent (3 ml) was heated to reflux under dinitrogen for 12 h. The reaction monitored by IR showed no new CO absorptions to indicate the formation of *mer*-$W(CO)_3(\eta^3$-PNN).

3.8. Co-pyrolysis of W(CO)$_6$ and PNN in a sealed tube

$W(CO)_6$ (23 mg) and PNN (21 mg) were mixed, ground, and sealed in a Pyrex glass tube under vacuum (0.01 torr). The tube was placed in a silicon oil bath at 125°C for 1 h, removed from oil bath and cooled to ambient temperature, and opened in air. The products were extracted with dichloromethane and crystallized by adding n-hexane. *fac*-$W(CO)_3(\eta^3$-PNN) (10%) and $W(CO)_4(\eta^2$-PNN) (23%) were obtained.

3.9. Structural determination for fac-W(CO)$_3$(η^3-PNN), fac-Mo(CO)$_3$(η^3-PNN) and W(CO)$_4$(η^2-PNN)

Crystals of *fac*-$W(CO)_3(\eta^3$-PNN) (ca. $0.60 \times 0.50 \times 0.20$ mm^3), *fac*-$Mo(CO)_3(\eta^3$-PNN) (ca. $0.50 \times 0.40 \times$

Table 3
Crystal data and refinement details for $W(CO)_4(\eta^2$-PNN), *fac*-$W(CO)_3(\eta^3$-PNN) and *fac*-$Mo(CO)_3(\eta^3$-PNN)

	$W(CO)_4$-(η^2-PNN)	$W(CO)_3$-(η^3-PNN)	$Mo(CO)_3$-(η^3-PNN)
Formula	$C_{30}H_{23}N_2O_4PW$	$C_{29}H_{23}N_2O_3PW$ CH_2Cl_2	$C_{29}H_{23}N_2O_3PMo$ CH_2Cl_2
Crystal solvent			
Formula weight	690.32	747.24	659.33
Temperature (K)	293(2)	293(2)	293(3)
Radiation λ (Å)	0.71073	0.71073	0.71073
Crystal system	Triclinic	Monoclinic	Monoclinic
Space group	$P\bar{1}$	$P2_1/n$	$P2_1/n$
Unit cell dimensions			
a (Å)	8.789(2)	13.400(2)	13.478(3)
b (Å)	10.533(2)	16.364(2)	16.390(4)
c (Å)	15.991(3)	13.602(2)	13.611(3)
α (°)	80.58(2)	90	90
β (°)	86.52(2)	102.02(1)	102.34(2)
γ (°)	68.73(2)	90	90
V (Å^3)	1361.0(5)	2917.3(6)	2937(1)
Z	2	4	4
$D_{calc.}$ (g cm^{-3})	1.685	1.701	1.491
$F(000)$	676	1464	1336
μ (mm^{-1})	4.341	4.232	0.717
R_1/wR_2 [a]	0.0197/0.0477	0.0290/0.0759	0.0421/0.1079
Goodness-of-fit on F^2	1.062	1.077	1.053

[a] $R_1 = \Sigma||F_o|-|F_c||/\Sigma|F_o|$; $wR_2 = \{\Sigma[w(|F_o|^2-|F_c|^2)^2]/\Sigma\, w|F_o|^4]\}^{1/2}$.

0.20 mm^3) and $W(CO)_4(\eta^2$-PNN) (ca. $0.60 \times 0.50 \times 0.50$ mm^3) were each mounted in a thin-walled glass capillary and aligned on the Nonius CAD-4 diffractometer with graphite-monochromated Mo–K_α radiation ($\lambda = 0.71073$ Å). The data were collected using the $\theta/2\theta$ scan technique with θ ranging from 1.94 to 25.00° for *fac*-$W(CO)_3(\eta^3$-PNN), 1.93 to 25.00° for *fac*-$Mo(CO)_3(\eta^3$-PNN) and 1.29 to 25.00° for $W(CO)_4(\eta^2$-PNN). All data were corrected for Lorentz and polarization effects and for the effects of absorption. The structures were solved by the heavy-atom method and refined by full-matrix least-square cycles on F^2 on the basis of 4232 observed reflections [$I > 2\sigma(I)$] for *fac*-$W(CO)_3(\eta^3$-PNN), 3612 observed reflections for *fac*-$Mo(CO)_3(\eta^3$-PNN) and 4438 observed reflections for $W(CO)_4(\eta^2$-PNN). The non-hydrogen atoms were refined anisotropically. Hydrogen atoms were included but not refined. All calculations were performed using the SHELXTL package. A summary of relevant crystallographic data is provided in Table 3.

4. Supplementary materials

Crystallographic data for the structural analysis has been deposited with the Cambridge Crystallographic Data Centre, CCDC nos. 136819 for $W(CO)_4(\eta^2$-PNN), 136817 for *fac*-$W(CO)_3(\eta^3$-PNN) and 136818 for *fac*-$Mo(CO)_3(\eta^3$-PNN). Copies of this information may be obtained free of charge from: The Director, CCDC, 12 Union Road, Cambridge, CB2 1EZ, UK (Fax: +44-1223-336033; e-mail: deposit@ccdc.cam.ac.uk or www: http://www.ccdc.cam.ac.uk).

Acknowledgements

We are grateful for support of this work by the National Science Council of Taiwan.

References

[1] A. Lavery, S.M. Nelson, J. Chem. Soc. Dalton Trans. (1984) 615.
[2] E. Drent, J.A.M. van Broekhoven, M.J. Doyle, J. Organomet. Chem. 417 (1991) 235.
[3] B.M. Trost, T.R. Verhoeven, J. Am. Chem. Soc. 100 (1978) 3435.
[4] G.W. Parshall, S.D. Ittel, Homogeneous Catalysis, Wiley, New York, 1992.
[5] F. Benvenuti, C. Carlini, M. Marchionna, R. Patrini, A.M. Raspolli Galletti, G. Sbrana, J. Mol. Catal. A Chem. 140 (1999) 139.
[6] R.E. Rülke, V.E. Kaasjager, P. Wehman, C.J. Elsevier, P.W.N.M. van Leeuwen, K. Vrieze, J. Fraanje, K. Goubitz, A.L. Spek, Organometallics 15 (1996) 3022.
[7] W.-Y. Yeh, C.-C. Yang, S.-M. Peng, G.-H. Lee, unpublished results.
[8] P. Wehman, R.E. Rülke, V.E. Kaasjager, P.C.J. Kamer, H. Kooijman, A.L. Spek, C.J. Elsevier, K. Vrieze, P.W.N.M. van Leeuwen, J. Chem. Soc. Chem. Commun. (1995) 331.
[9] T.B. Rauchfuss, J. Organomet. Chem. 162 (1978) C19.
[10] F.A. Cotton, G. Wilkinson, Advanced Inorganic Chemistry, fifth ed., Wiley, New York, 1988.
[11] F. Basolo, Polyhedron 9 (1990) 1503.
[12] D.M.P. Mingos, J. Organomet. Chem. 179 (1979) C29.
[13] S.C.N. Hsu, W.-Y. Yeh, J. Chem. Soc. Dalton Trans. (1998) 125.
[14] P.E. Garrou, Chem. Rev. 81 (1981) 229.
[15] D.F. Shriver, M.A. Drezdzon, The Manipulation of Air-Sensitive Compounds, second ed., Wiley, New York, 1986.
[16] D.D. Perrin, W.L. Armarego, D.R. Perrin, Purification of Laboratory Chemicals, Pergamon, Oxford, 1966.